

## DNA Replication

International Edition: DOI: 10.1002/anie.201606137  
German Edition: DOI: 10.1002/ange.201606137

## Ion-Mediated Polymerase Chain Reactions Performed with an Electronically Driven Microfluidic Device

Yi Zhang<sup>†</sup>, Qian Li<sup>†</sup>, Linjie Guo, Qing Huang, Jiye Shi, Yang Yang, Dongsheng Liu,\* and Chunhai Fan\*

**Abstract:** The polymerase chain reaction (PCR) is a powerful method for exponentially amplifying very low amounts of target DNA from genetic, clinical, and forensic samples. However, the heating and cooling steps in PCR largely hamper the miniaturization of thermocyclers for on-site detection of pathogens and point-of-care tests. Herein, we devise an ion-mediated PCR (IM-PCR) strategy by exploiting ion-induced DNA denaturation/renaturation cycles. DNA duplexes are effectively denatured in alkaline solutions; whereas, the denatured single-stranded DNA strands readily reform duplexes at neutral pH. By using an integrated microchip that can programmably control the solution pH simply switching the potential in a range of several hundred millivolts, we can trigger IM-PCR at a constant temperature. Analogously to thermal cycling, 30 cycles of pH-induced denaturation/renaturation were used to amplify protein DNA fragments as confirmed by DNA sequencing. We anticipate that this portable, low-cost, and scalable IM-PCR holds great promise for widespread biological, clinical, and environmental applications.

The polymerase chain reaction (PCR), originally invented in 1983 by Mullis, is an important and standard technique in molecular biology.<sup>[1]</sup> As a mimic of the natural DNA replication machine, PCR uses a DNA polymerase to

synthesize new strands of DNA complementary to the given template strand in vitro, which in turn are used as templates for replication to initiate a chain reaction upon temperature cycling.<sup>[2]</sup> Because of its extraordinarily high ability to amplify very low amounts of specific nucleic acid sequences from the large background of the genome, PCR and its variants have found widespread applications including clinical diagnosis, genetic and forensic analysis, and bioterrorism prevention and preparedness.<sup>[3]</sup>

Unlike DNA replication in vivo, which uses a set of enzymes/proteins to separate the DNA double helix, currently available PCR relies on thermal melting to denature the DNA duplex for replication.<sup>[1]</sup> In its original version, the repeated heating and cooling cycles were operated manually. This cumbersome procedure was later replaced with automatic thermal cyclers. After decades of academic and industrial efforts, state-of-the-art thermal cyclers can provide relatively uniform temperature and rapid heating-cooling cycles and avoid water condensation, which has overcome many problems that might have been encountered in laboratory and clinical settings.<sup>[4]</sup> With these advances, the commercialization of PCR has proven extremely successful in many areas.<sup>[5]</sup> Nevertheless, the high cost and large size of thermal cyclers hamper their applications in resource-limited situations. Great efforts have been taken to miniaturize PCR devices, for example, using Rayleigh-Bénard convective cells, which have yet to achieve the full functions of commercial thermal cyclers.<sup>[6]</sup> In particular, the lag phase in heating-cooling cycling and inhomogeneous temperature distribution in the solution are difficult to avoid in these simple designs.<sup>[7]</sup>

Hydrogen bonds in DNA duplexes are sensitive to low or high solution pH.<sup>[8]</sup> Therefore, pH variation can in principle denature/renature DNA duplexes to trigger chain reactions in a similar way to temperature cycling.<sup>[9]</sup> However, this alternative approach has not been explored to amplify nucleic acids, which possibly is due to the predominant use of thermal cycling for historical reasons that restrict explorations in other directions.<sup>[10]</sup> Moreover, changing the solution pH in an automated way is difficult. Herein, we develop an ion-mediated PCR (IM-PCR) strategy to amplify nucleic acids with pH cycling at a constant temperature (Scheme 1). By using an electronically-driven microfabricated chip that can automatically tune the proton-hydroxide-ion equilibrium in solution using potential control, we have achieved automated DNA denaturation/renaturation and specific target amplification, which paves the way to electronically-driven PCR that could be potentially integrated with electronic DNA sequencing.<sup>[8c,9b]</sup>

[\*] Dr. Y. Zhang,<sup>[†]</sup> Prof. Q. Li,<sup>[†]</sup> L. Guo, Prof. Q. Huang, Prof. C. Fan  
Division of Physical Biology & Bioimaging Center, Shanghai  
Synchrotron Radiation Facility, CAS Key Laboratory of Interfacial  
Physics and Technology, Shanghai Institute of Applied Physics,  
Chinese Academy of Sciences  
Shanghai 201800 (China)  
E-mail: fchh@sinap.ac.cn

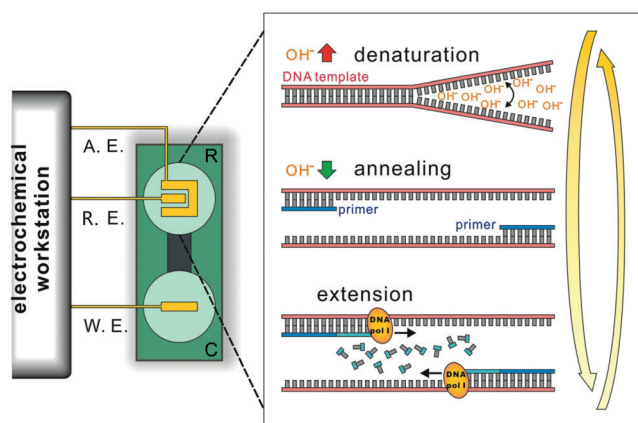
Dr. J. Shi  
Kellogg College, University of Oxford  
Oxford, OX2 6PN (UK)  
and  
UCB Pharma  
208 Bath Road, Slough, SL1 3WE (UK)

Dr. Y. Yang  
National Center for NanoScience and Technology (NCNST)  
Beijing 100190 (China)

Prof. D. Liu  
Key Laboratory of Organic Optoelectronics & Molecular Engineering  
of the Ministry of Education, Department of Chemistry  
Tsinghua University  
Beijing 100084 (China)  
E-mail: liudongsheng@mail.tsinghua.edu.cn

[†] These authors contributed equally to this work.

Supporting information for this article can be found under:  
<http://dx.doi.org/10.1002/anie.201606137>.



**Scheme 1.** Illustration of the working principle of IM-PCR. In the denaturation step, hydrogen bonds between complementary bases of DNA templates are disrupted under high pH. The solution pH is then made neutral, which allows primer annealing to the template and subsequent replication in the presence of DNA polymerase. This IM-PCR process can be performed in an automated electronically-driven microfabricated device that incorporates a pH-sensitive  $\text{IrO}_x$  reference electrodes (R.E.), a Ag/AgCl working electrode (W.E.), and an Ir auxiliary electrode (A.E.). Reaction region (R) and control region (C) are filled with 0.1 M KCl.

We first studied the pH effect on DNA melting at room temperature by employing a piece of 120-bp double-stranded (ds) DNA fragment T1 as the template (Supporting Information, Table S1). DNA bases tend to lose purines in the low pH range of 0–3, whereas DNA is usually stable in the high pH range of 12–13 without detectable damage in a relatively short period (for example, in a standard genetic comet assay).<sup>[11]</sup> Therefore, we mainly studied the high pH region of 11–13. A Britton-Robinson (BR) buffer system that covers a wide range of pH values from 2 to 12 was employed to vary the solution pH.<sup>[12]</sup> The dsDNA was first incubated in solutions with an alkaline pH for 60 s and then renatured at pH 7 for 30 s. The renaturation products were analyzed using agarose gel electrophoresis (AGE) (Supporting Information, Figure S1). As expected, renaturation of dsDNA in BR buffer resulted in the appearance of the 120-bp dsDNA band in the gel, which suggests that the dsDNA denaturation/renaturation is reversible. To further substantiate the reversibility of the DNA denaturation/renaturation, we designed a DNA hybridization-specific fluorescent probe (FP) (Supporting Information, Table 1). A fluorophore–quencher pair of 6-carboxyfluorescein (FAM) and Black Hole Quencher-1 (BHQ1) was used to label the 5'- and 3'- ends of the DNA strands, as illustrated in Figure 1a. In the dsDNA state, FAM and BHQ1 are held together, which enables efficient energy-transfer-based fluorescence quenching.<sup>[13]</sup> Denaturation of dsDNA at pH 12 separates the two strands and the attached FAM and BHQ1 labels, resulting in the appearance of the FAM fluorescence.<sup>[14]</sup> As shown in Figure 1a, we observed nearly reversible On and Off states of FAM fluorescence upon switching the solution pH between 7 and 12 over 10 cycles. These quantitative fluorescence data provide further evidence for pH-induced denaturation/renaturation cycles as observed in the gel studies.

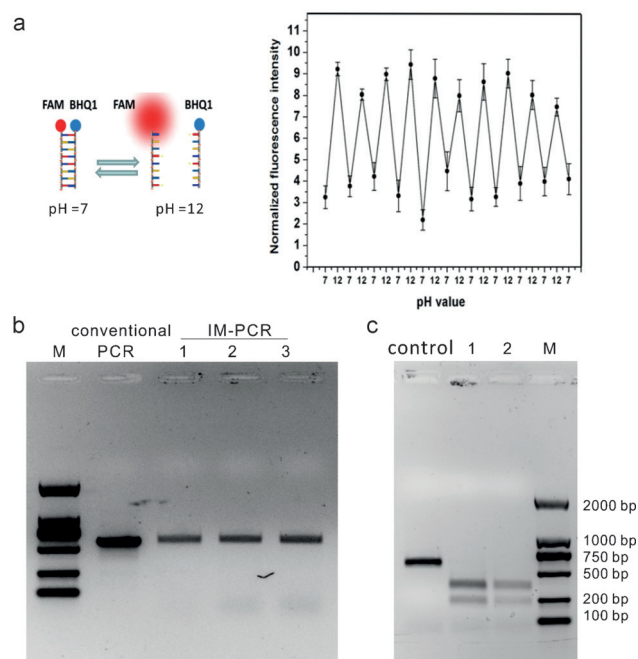


**Figure 1.** a) pH-induced reversible denaturation/renaturation of a 20-bp DNA fluorescent probe F1 as revealed by FAM fluorescence. b) Comparison of 30-cycle conventional PCR and IM-PCR of a 571-bp mCherry protein fragment T2. Three independent IM-PCR experiments are shown in lanes 1, 2, and 3. The gel image was over exposed to visualize the band of primers. c) Enzymatic restriction analysis of thermally-driven PCR and IM-PCR products: 571-bp template T2 (control), enzyme restriction products of conventional PCR products (lane 1) and IM-PCR products (lane 2), DNA marker DL2000 (M).

Having established the reversibility and robustness of pH-induced denaturation/renaturation of DNA duplexes, we next tested whether this pH melting could trigger chain reactions for nucleic acid amplification. A 571-bp fragment of mCherry protein T2 (Supporting Information, Table S1) was employed as the template for IM-PCR amplification. In the first denaturation step, the template was incubated in 50  $\mu\text{L}$  of BR buffer at pH 12 for 60 s at 37°C, which contained primers, deoxyribonucleoside triphosphate (dNTPs), and  $\text{Mg}^{2+}$ , which are essential for DNA replication. The solution pH was tuned to 7 by adding aliquots of BR buffer of pH 2, and the solution was incubated for 20 s for renaturation. After that, an aliquot containing DNA polymerase I (Pol I) was added to the solution to allow a 40-sec extension step. These procedures were performed manually for 30 cycles. During each cycle, fresh Pol I was added to ensure continuous replication. After 30 cycles of manual amplification using IM-PCR, we analyzed the product using AGE and observed a specific band corresponding to the 571-bp fragment (Figure 1b). The bands were essentially in the same position as that obtained from conventional thermally-driven PCR, which suggests that we have amplified the target DNA fragment successfully. We also note that the yields of manually performed IM-PCR are lower than that from conventional PCR (Figure 1b), which results from a combination of factors, including the volume fluctuation of the reaction solution and non-optimal conditions for DNA polymerase I.

We further tested the specificity of IM-PCR amplification by using an enzymatic restriction assay and DNA sequencing of the product. The target DNA fragment contains a specific site for Hinf-I endonuclease. We incubated the amplified fragment with Hinf-I and analyzed digestion products with AGE. Both thermally-driven PCR and IM-PCR showed similar results (Figure 1c). DNA sequencing of the products performed by Sangon Biotech (Shanghai, China) using capillary electrophoresis further confirms specific amplification without detectable errors in IM-PCR. Control studies also showed that IM-PCR was initiated only in the presence of both the template and dNTPs (Supporting Information, Figure S2). The absence of either component did not generate any detectable product.

The success in manual IM-PCR motivated us to explore programmable nucleic acid amplification with electronically-driven automated variation of the solution pH. We employed an electronically-driven microfabricated device consisting of a three-electrode chip with photolithographically fabricated Ir, IrO<sub>x</sub>, and Ag/AgCl electrodes and a polydimethylsiloxane (PDMS) chamber (around 10 × 20 mm<sup>2</sup>) (Supporting Information, Figure S3). This microfabricated electronic chip is a pH-stat with negative feedback.<sup>[9a]</sup> Because the IrO<sub>x</sub> reference electrode (R.E.) is pH-sensitive, the potential between the Ag/AgCl working electrode (W.E.) and the R.E. has a direct relationship with the pH in the response/reaction region (R region) around the R.E. and the Ir auxiliary electrodes (A.E.). Calibration of the device was performed by titrating a series of BR buffers with pH 4 to 12 using the open circuit potential (OCP) method (Supporting Information, Figure S4). As shown in Figure 2a, the potential between W.E. and R.E. changed with the solution pH, generating a linear relationship with a slope of 48 mV pH<sup>-1</sup>. Therefore, we can precisely and automatically adjust the solution pH by simply applying the appropriate potentials to the W.E. The potentials of −3 mV and −243 mV corresponded to pH 12 and pH 7, respectively. We also note that the response time for the pH change is less than 2 s (Figure 2b).

Having established the electronic chip for digital pH response, we employed it for the automated pH alternation of an IM-PCR solution. A 100 μL aliquot of a solution containing T1, primers, dNTPs, and Mg<sup>2+</sup> was loaded into the reaction region of the chamber. The potential was first set to −3 mV (corresponding to pH 12) for 30 s. During this period, a negative current of approximately 60 μA was observed, which rapidly decayed to approximately 10<sup>−3</sup> μA within 2 s and remained in this steady state (Figure 2b). Then the potential was switched to −243 mV (corresponding to pH 7) and held for 30 s, a positive current appeared instantly, decayed rapidly, and remained steady again (Figure 2b). These data clearly suggested that the pH change in the IM-PCR reaction solution in R region was rapid and could be stabilized at the desired values. To further substantiate the robustness of the pH alternation, we recorded the pH-induced reversible denaturation/renaturation of the FP on the chip. As shown in Figure 2c and the Supporting Information, Figure S5, the potential between the R.E. and W.E. was set to −3 (corresponding to pH 12) and −243 mV (corresponding to

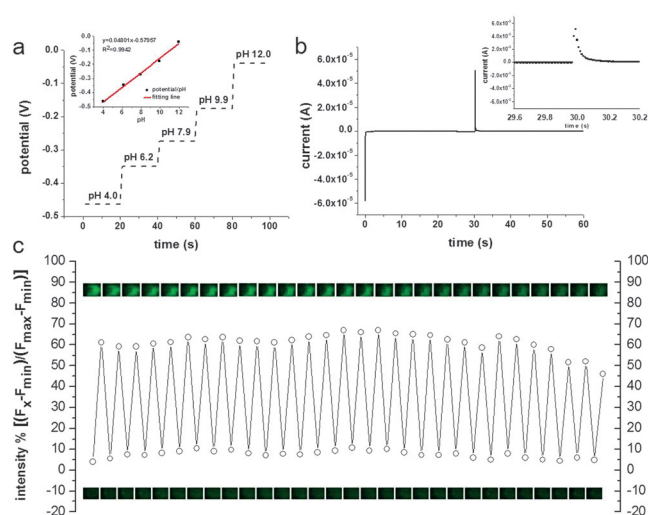


**Figure 2.** Performance of the electronically driven microfabricated chip. a) OCP-based calibration of the chip using BR buffer with pH 2–12. b) Chronoamperometric responses upon setting the potential at −3 mV (pH 12) for 30 s and −243 mV (pH 7) for 30 s. c) The fluorescence intensity changes of the FP solution in the R region over 30 cycles manipulated by alternating the operation potentials between −3 and −243 mV with 30 s per step.

pH 7) alternatively every 30 s, which switched the fluorescence on and off almost instantly, over 30 cycles. This result clearly demonstrates that pH alternation in the R region of the chip is fast and robust, which indicates that the device was capable of triggering pH variation in IM-PCR.

We then employed the electronic chip for automated electronically driven IM-PCR (EDIM-PCR) amplification of target DNA pieces by loading 100 μL of solutions containing primers, dNTPs, and Mg<sup>2+</sup> into the chamber. The amplification using EDIM-PCR was performed at ambient temperature. Although a higher temperature would increase the processivity of the polymerase, heating of the chip evaporates liquid in the chamber and probably affects the electrochemistry. We found that DNA polymerase I (Pol I) had a higher activity than Taq under these conditions (Supporting Information, Figure S6). The potential was switched between −3 mV (pH 12) and −243 mV (pH 7). After 30 cycles of EDIM-PCR with Pol I, we analyzed the product using AGE and found the correctly amplified product. As indicated in Figure 3, DNA products with comparable molecular weights were obtained. The product from EDIM-PCR was further verified by amplifying it in a thermal cycler, which generated a product with the same band position. Capillary sequencing of the EDIM-PCR product by Sangon Biotech (Shanghai, China) confirmed that we had obtained the correct amplified fragment.

Denaturation of the double helix is a key step for in vitro replication of nucleic acids, which can be triggered by thermal melting, pH variation, or the presence of denaturants. Thermal melting has been predominantly used in PCR amplification. This is a green approach essentially free of the addition of chemicals. Since dsDNA is known to denature in solutions of low or high pH values, owing to the disruption of hydrogen bonds between complementary bases, pH



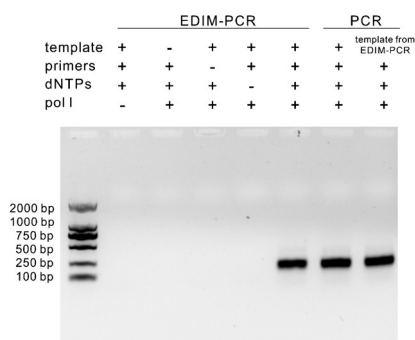


**Figure 3.** Agarose gel electrophoresis analysis of EDIM-PCR products of 120-bp T1. Lanes 1 to 4: EDIM-PCR solution without DNA polymerase, template, primers or dNTPs, respectively; lane 5: EDIM-PCR products; lane 6: conventional PCR products; lane 7: conventional PCR products using the template amplified by EDIM-PCR. M: DNA marker DL2000.

variation-induced denaturation is a promising alternative that changes only the concentrations of protons and hydroxide ions in solution.<sup>[11,15]</sup> Specifically, we find that switching between alkaline and neutral solutions can reversibly denature and renature DNA duplexes in a robust way. Similar to thermal cycling in conventional PCR, repetitive cycling of the solution pH forms the principle of IM-PCR for DNA amplification. Alkaline denaturation is a mild approach for DNA operations. For example, reversible alkaline denaturation has been used in standard biological assays, including Illumina sequencing sample preparation. Furthermore, DNA sequencing confirmed that the correct products, without detectable errors, were obtained using pH-induced PCR.

Since the invention of PCR, many new versions of nucleic acid amplification have appeared. In particular, isothermal amplification has been developed to overcome the problems associated with temperature cycling in PCR.<sup>[16]</sup> However, these isothermal approaches typically employ novel mechanisms that are different than conventional PCR, which involve either the use of multiple enzymes or replace exponential amplification with linear amplification.<sup>[16]</sup> The IM-PCR described in this work relies on a single polymerase and does not modify the exponential amplification mechanism of PCR. Therefore, the replacement of temperature cycling with pH cycling represents a novel approach for isothermal amplification. Electrically driven pH-cycling is performed at ambient temperature with a low potential of several hundred millivolts. Notably, such low potentials are much lower than the redox potential of the DNA bases, which makes them amenable for DNA operations.<sup>[17]</sup> The fabrication of the microfluidic device uses conventional fabrication processes and is fully compatible with the electronics industry. Therefore, it is possible to develop portable and low-cost PCR devices for high-throughput analysis by using lithography-based multi-channel systems driven by small-sized electronics.

Despite these advantages, we also note that the amplification efficiency of EDIM-PCR is lower than that of conventional PCR. The main reason is likely the lack of appropriate polymerases that are analogous to Taq, which works optimally

at high temperature in thermal cyclers. Both Taq and Pol I have low activities at alkaline pH, which greatly restrict the amplification efficiency. It is envisioned that exploration of bacteria living in the alkaline environments or directed evolution of polymerases might lead to the discovery of polymerases suitable for working with IM-PCR.<sup>[18]</sup> The inefficiency of IM-PCR may also result from the low temperature, alkaline-mediated damage to PCR ingredients, or the open-chamber configuration of the EDIM-PCR device. We anticipate that optimization and sealing of the electronic chip will generate a novel PCR device with performance comparable or superior to that of thermal cyclers, which should open new opportunities for low-cost and portable PCR detection in resource-limited settings.

In summary, we have developed an electrically driven ion-mediated PCR strategy for dsDNA amplification by employing an integrated electronic microfluidic chip. We have demonstrated that pH changes of reaction solution could serve as the trigger for PCR amplification, which opens new opportunities for improving PCR.

## Acknowledgements

This work was financially supported by the National Basic Research Program of China (973 Program, 2012CB825805, 2012CB932603, 2013CB933800) and the National Natural Science Foundation of China (21505148, 21390414, 21227804, 61378062, and 21534007).

**Keywords:** dna amplification · isothermal PCR · microfluidic devices · pH cycling · pH-stats

**How to cite:** *Angew. Chem. Int. Ed.* **2016**, 55, 12450–12454  
*Angew. Chem.* **2016**, 128, 12638–12642

- [1] R. K. Saiki, S. Scharf, F. Faloona, K. B. Mullis, G. T. Horn, H. A. Erlich, N. Arnheim, *Science* **1985**, 230, 1350–1354.
- [2] R. K. Saiki, D. H. Gelfand, S. Stoffel, S. J. Scharf, R. Higuchi, G. T. Horn, K. B. Mullis, H. A. Erlich, *Science* **1988**, 239, 487–491.
- [3] a) S. Michalatos-Beloin, S. A. Tishkoff, K. L. Bentley, K. K. Kidd, G. Ruano, *Nucleic Acids Res.* **1996**, 24, 4841–4843; b) S. A. Bustin, R. Mueller, *Clin. Sci.* **2005**, 109, 365–379; c) S. Wuertz, M. Belay, F. Kirschbaum, *Aquaculture* **2007**, 269, 130–134; d) K. J. M. Jeffery, S. J. Read, T. E. A. Peto, R. T. Mayon-White, C. R. M. Bangham, *Lancet* **1997**, 349, 313–317; e) A. Alonso, P. Martín, C. Albarrán, P. García, O. García, L. F. de Simón, J. García-Hirschfeld, M. Sancho, C. de La Rúa, J. Fernández-Piqueras, *Forensic Sci. Int.* **2004**, 139, 141–149.
- [4] G. C. Saunders, J. Dukes, H. C. Parkes, J. H. Cornett, *Clin. Chem.* **2001**, 47, 47–55.
- [5] a) P. Belgrader, S. Young, B. Yuan, M. Primeau, L. A. Christel, F. Pourahmadi, M. A. Northrup, *Anal. Chem.* **2001**, 73, 286–289; b) E. K. Wheeler, W. Benett, P. Stratton, J. Richards, A. Chen, A. Christian, K. D. Ness, J. Ortega, L. G. Li, T. H. Weisgraber, K. Goodson, F. Milanovich, *Anal. Chem.* **2004**, 76, 4011–4016.
- [6] a) M. Krishnan, V. M. Ugaz, M. A. Burns, *Science* **2002**, 298, 793; b) G. Ahlers, S. Grossmann, D. Lohse, *Rev. Mod. Phys.* **2009**, 81, 503–537.
- [7] Q. Xiang, B. Xu, R. Fu, D. Li, *Biomed. Microdevices* **2005**, 7, 273–279.

- [8] a) M. Ageno, E. Dore, C. Frontali, *Biophys. J.* **1969**, *9*, 1281–1311; b) K. Klepárník, Z. Malá, P. Boček, *Electrophoresis* **2001**, *22*, 783–788; c) Z. Malá, K. Klepárník, P. Boček, *J. Chromatogr. A* **1999**, *853*, 371–379; d) T. Osafune, H. Nagata, Y. Baba, *Anal. Sci.* **2004**, *20*, 971–974; e) J. M. Rothberg, W. Hinz, T. M. Rearick, J. Schultz, W. Mileski, M. Davey, J. H. Leamon, K. Johnson, M. J. Milgrew, M. Edwards, J. Hoon, J. F. Simons, D. Marran, J. W. Myers, J. F. Davidson, A. Branting, J. R. Nobile, B. P. Puc, D. Light, T. A. Clark, M. Huber, J. T. Branciforte, I. B. Stoner, S. E. Cawley, M. Lyons, Y. Fu, N. Homer, M. Sedova, X. Miao, B. Reed, J. Sabina, E. Feierstein, M. Schorn, M. Alanjary, E. Dimalanta, D. Dressman, R. Kasinskas, T. Sokolsky, J. A. Fidanza, E. Namsaraev, K. J. McKernan, A. Williams, G. T. Roth, J. Bustillo, *Nature* **2011**, *475*, 348–352.
- [9] a) Y. Yang, G. Liu, H. Liu, D. Li, C. Fan, D. Liu, *Nano Lett.* **2010**, *10*, 1393–1397; b) C. Toumazou, L. M. Shepherd, S. C. Reed, G. I. Chen, A. Patel, D. M. Garner, C. J. Wang, C. P. Ou, K. Amin-Desai, P. Athanasiou, H. Bai, I. M. Brizido, B. Caldwell, D. Coomber-Alford, P. Georgiou, K. S. Jordan, J. C. Joyce, M. La Mura, D. Morley, S. Sathyavrudhan, S. Temelso, R. E. Thomas, L. Zhang, *Nat. Methods* **2013**, *10*, 641–646.
- [10] a) A. J. Hoff, A. L. M. Roos, *Biopolymers* **1972**, *11*, 1289–1294; b) H. C. Birnboim, J. Doly, *Nucleic Acids Res.* **1979**, *7*, 513–1523; c) A. M. Maxam, W. Gilbert, *Proc. Natl. Acad. Sci. USA* **1977**, *74*, 560–564; d) A. M. Maxam, W. Gilbert, *Methods Enzymol.* **1980**, *65*, 499–560; e) K. Morimoto, M. Toya, J. Fukuda, H. Suzuki, *Anal. Chem.* **2008**, *80*, 905–914; f) A. A. Shaikh, J. Firdaws, S. Serajee, M. S. Rahman, P. K. Bakshi, *Int. J. Electrochem. Sci.* **2011**, *6*, 2333–2343.
- [11] H. Erlenmeyer, R. Griesser, B. Prijs, H. Sigel, *Biochim. Biophys. Acta Nucleic Acids Protein Synth.* **1968**, *157*, 637–640.
- [12] T. T. Herskovits, *Biochemistry* **1963**, *2*, 335–340.
- [13] M. K. Johansson, H. Fidler, D. Dick, D. R. M. Cook, *J. Am. Chem. Soc.* **2002**, *124*, 6950–6956.
- [14] U. V. Schneider, J. K. Severinsen, I. Géci, L. M. Okkels, N. Jøhnk, N. D. Mikkelsen, T. Klinge, E. B. Pedersen, H. Westh, G. Lisby, *BMC Biotechnol.* **2010**, *10*:4.
- [15] H. C. Birnboim, *Methods Enzymol.* **1983**, *100*, 243–255.
- [16] a) Y. Zhao, F. Chen, Q. Li, L. Wang, C. Fan, *Chem. Rev.* **2015**, *115*, 12491–12545; b) L. Yan, J. Zhou, Y. Zheng, A. S. Gamson, B. T. Roembke, S. Nakayama, H. O. Sintim, *Mol. Biosyst.* **2014**, *10*, 970–1003; c) D. Liu, S. L. Daubendiek, M. A. Zillman, K. Ryan, T. K. Kool, *J. Am. Chem. Soc.* **1996**, *118*, 1587–1594; d) N. Tomita, Y. Mori, H. Kanda, T. Notomi, *Nat. Protoc.* **2008**, *3*, 877–882; e) Y. Tian, Y. Wang, Y. Xu, Y. Liu, D. Li, C. Fan, *Sci. China Ser. B* **2015**, *58*, 514–518.
- [17] a) F. Boussicault, M. Robert, *Chem. Rev.* **2008**, *108*, 2622–2645; b) E. Palecek, M. Bartošík, *Chem. Rev.* **2012**, *112*, 3427–3481.
- [18] a) G. S. Roadcap, R. A. Sanford, Q. Jin, J. R. Pardinas, C. M. Bethke, *Ground Water* **2006**, *44*, 511–517; b) A. Fahy, A. S. Ball, G. Lethbridge, K. N. Timmis, T. J. McGenity, *Lett. Appl. Microbiol.* **2008**, *47*, 60–66; c) S. Suzuki, J. G. Kuenen, K. Schipper, S. van der Velde, Sh. Ishii, A. Wu, D. Y. Sorokin, A. Tenney, X. Meng, P. L. Morrill, Y. Kamagata, G. Muyzer, K. H. Nealson, *Nat. Commun.* **2014**, *5*, 3900; d) L. Preiss, D. B. Hicks, S. Suzuki, T. Meier, T. A. Krulwich, *Front. Bioeng. Biotechnol.* **2015**, *3*, 75.

Received: June 24, 2016

Revised: July 19, 2016

Published online: September 9, 2016